Computational and Mathematical Methods in Medicine

Correlation of mechanical factors and gallbladder pain

W. G. Li [a]; X. Y. Luo [b]; N. A. Hill [b]; A. Smythe [c]; S. B. Chin [a]; A. G. Johnson [c]; N. Bird [c]

[a] Department of Mechanical Engineering, University of Sheffield, Sheffield, UK
[b] Department of Mathematics, University of Glasgow, Glasgow, UK
[c] Academic Surgical Unit, Royal Hallamshire Hospital, Sheffield, UK

PLEASE SCROLL DOWN FOR ARTICLE

Taylor & Francis
Taylor & Francis Group

Correlation of mechanical factors and gallbladder pain

W. G. LI†, X. Y. LUO*‡, N. A. HILL‡, A. SMYTHE¶, S. B. CHIN†, A. G. JOHNSON¶ and N. BIRD¶

†Department of Mechanical Engineering, University of Sheffield, Sheffield S1 3JD, UK
‡Department of Mathematics, University of Glasgow, Glasgow G12 8QW, UK
¶Academic Surgical Unit, Royal Hallamshire Hospital, Sheffield S10 2JF, UK

Acalculous biliary pain occurs in patients with no gallstones, but is similar to that experienced by patients with gallstones. Surgical removal of the gallbladder (GB) in these patients is only successful in providing relief of symptoms to about half of those operated on, so a reliable pain-prediction model is needed. In this paper, a mechanical model is developed for the human biliary system during the emptying phase, based on a clinical test in which GB volume changes are measured in response to a standard stimulus and a recorded pain profile. The model can describe the bile emptying behaviour, the flow resistance in the biliary ducts, the peak total stress, including the passive and active stresses experienced by the GB during emptying. This model is used to explore the potential link between GB pain and mechanical factors. It is found that the peak total normal stress may be used as an effective pain indicator for GB pain. When this model is applied to clinical data of volume changes due to Cholecystokinin stimulation and pain from 37 patients, it shows a promising success rate of 88.2% in positive pain prediction.

Keywords: Gallbladder; Total stress; Gallbladder pain; Gallstone; Flow resistance; Emptying

1. Introduction

Human gallbladder (GB) pain is typically described as pain in the right upper part of the abdomen lasting for 30 min or more and provoked by a fatty meal, but not all patients experience these classical symptoms. Gallstones are the common cause, but only a small minority of the 10% of the population with stones experience pain. GB pain, also known as acalculous biliary or functional biliary pain, is defined as a steady pain located in the epigastrium and right upper quadrant in the absence of gallstones or when no other structural abnormalities exist in the biliary tract [1]. This pain may occur up to 7.6% in men and 20.7% in women, and has received great interest in recent years [2,3]. Patients with GB pain often pose diagnostic difficulties and undergo repeated ultrasound scans and oral cholecystograms. Sonography (oral cholecystography) combined with scintigraphy is commonly used to diagnose GB pain. Reproduction of pain within 5–10 min of an injection of cholecystokinin (CCK) is also used to select a group of patients who may benefit from cholecystectomy [4].

However, surgery is often conducted without any guarantee of relieving the symptoms. Previous attempts to provide an accurate predictor for relief of GB symptoms have not been successful with only about 50% of patients obtaining symptomatic relief following surgery [5]. Moreover, some patients without stones appear to have typical GB pain, but only half of them gain relief of their pain if the GB is removed. It is therefore important to have a way of determining whether the pain is actually arising in the GB, because similar symptoms can be produced by adjacent organs, such as the stomach, duodenum and pancreas, even without obvious disease.

Impaired motor function of GB and sphincter of Oddi has long been suspected to be a major factor contributing to GB pain. The presumed mechanism for the pain is obstruction leading to distension and inflammation. The obstruction might result from a lack of co-ordination between the GB and either the cystic duct or the sphincter of Oddi due to increased flow resistance or tone [2]. In other words, pain may be produced by contraction against resistance or stretch of the GB wall. When the GB is inflamed, artificial distension produces GB pain [6].

The pain provocation test has been used as a diagnostic tool to select patients with impaired GB motor function who may benefit from the cholecystectomy. In the test CCK is injected intravenously to stimulate the GB to contract and to induce the biliary pain. It is clinically accepted that when a GB ejection fraction (percentage of the volume displaced during emptying) is less than 35% [7] or 40% [8], then the GB motor function is considered to be impaired; otherwise, it is considered normal. It has been found that the GB pain of some patients has been alleviated after their GBs are removed [7,8]. However, conflicting reports also exist [3,5,9]. These facts suggest that impaired GB motor function is not the only factor responsible for the pain.

As a type of visceral pain, GB pain arises from the GB and biliary tract with obstruction of the cystic or common bile ducts, which elevates pressure within the biliary system. Some researchers believe that the pain is directly related to intraluminal pressure of the biliary tract [10]. Gaensler (1951) examined the pain threshold of common bile duct for 40 patients before and after GB removal. It was found that the pain threshold varied from 14.7 to 59 mmHg [11]. Csendes *et al.* (1979) illustrated that the pain threshold is in the range 15–60 mmHg [12]. The great variation in the pressure range in these studies suggests that the sensor of the pain in the biliary system may be better associated with other mechanical factors associated with the intraluminal pressure, but not directly to the pressure alone. Similar observations were made for pain in the oesophagus, duodenum, gastric antrum and rectum, which seems to respond to mechanoreceptors in the gastrointestinal tract wall [13]. These mechanoreceptors are found to depend on the luminal circumferential wall strain rather than pressure, tension and volume [13–17].

In this paper, we study GB pain from the mechanical point of view, i.e. the human biliary system is considered as a pressure-flow dynamic system with a flexible wall. By estimating and comparing different mechanical factors from a group of patients, we were able to identify that the peak normal stress is the single most significant mechanical factor related to the pain felt by these patients. When this is used for pain prediction, a promising 88.2% positive correlation is achieved with the clinical observations of pain for 37 patients at the Academic Surgical Unit of the Royal Hallamshire Hospital at Sheffield, UK. We emphases that this new pain predictor can be derived from *non-invasive* measurements of geometry changes during the emptying, thus it may feasibly serve as an aid for real-time clinical diagnosis.

2. Model and method

2.1 Acquisition of clinical data during emptying

A CCK provocation test was carried on patients who had experienced repeated attacks of biliary-type pain in the absence of gallstones or any obvious causative findings [18]. After an overnight fast, they were given an intravenous infusion of saline (control) followed by an intravenous infusion of CCK (0.05 µg/kg body weight). Ultrasonography of the GB was used to monitor changes in shape, initial volume, emptying and wall thickness at 15 min intervals for 60 min. Note that pressure is not recorded in the experiments, which would require invasive techniques. The values of pressure for different subjects are predicted using the mechanical model (below) based on the volume and shape changes measured. The patients were unaware of which substance was being given and the test was only considered positive when the patients' usual "gallbladder" pain was reproduced following CCK infusion.

Figure 1 illustrates schematically the pressure and volume variation with time during CCK provocation test. At point 1, the sphincter of Oddi is closed (see figure 2), the GB is in a fasting state, and its volume, pressure and stresses all reach their minimum levels. Between 1 and 2, a small but positive pressure difference between the liver and the GB exists, which allows the hepatic bile to be secreted slowly into the GB. During this refilling, although, the GB volume is increasing, the pressure in GB is more or less constant as the muscle relaxes. This is because the production of hepatic bile is low pressure (typically 10 mmHg or less), continuous and easily halted by any rise in pressure in the GB or common bile duct [19]. At point 2, CCK is infused, which causes the GB to contract. The pressure in the GB rises rapidly up to point 3 in 3–5 min, and exceeds the pressure in the common bile duct. During
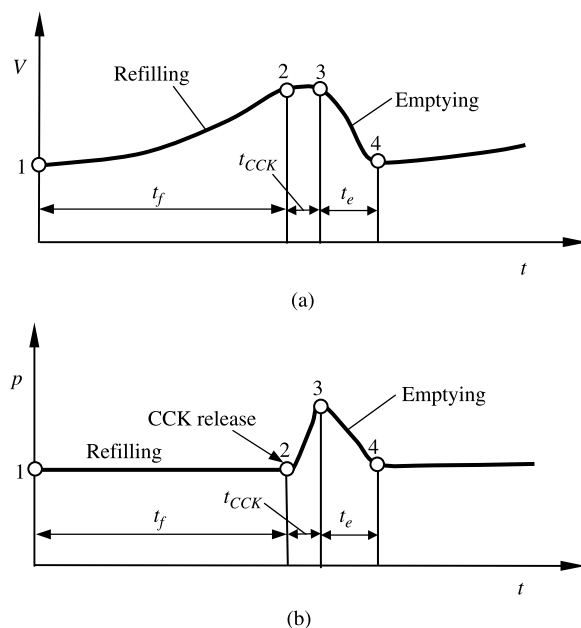

Figure 1. Diagrammatic representation of GB refilling and emptying. Refilling starts at point 1 and stops at point 2. Emptying begins at point 2 and lasts until point 4, when the next refilling starts. Note t_f is the refilling time t_e is the emptying time, and $t_f \approx 6t_e$.
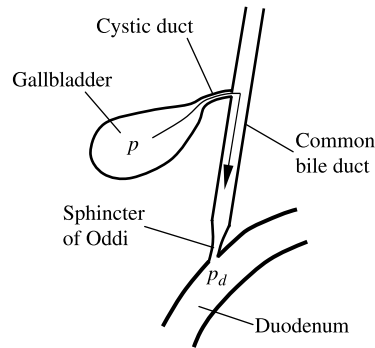
Figure 2. Bile flows into the duodenum from the GB through the cystic and common bile ducts due to the pressure difference $p - p_{\mathrm{d}}$.

this time, the sphincter of Oddi relaxes which lowers the pressure in the common bile duct further. The relative pressure in the GB is now much higher than the common bile duct, and the emptying phase takes place. For most of the subjects, this lasts for about half an hour. The time scale for refilling is usually the time lapse between two meals and is often more than six times longer than emptying.

2.2 Mechanical modelling

2.2.1 Predicting the pressure in gallbladder. GB emptying is caused by passive and active contractions due to the relaxation of stretch and CCK stimulation. The flow configuration in a biliary system is indicated in figure 2. During emptying, the bile flow rate out of the GB, Q_{GB} ($= -\mathrm{d}V/\mathrm{d}t$), is equal to the flow rate into the duct, Q_{duct}, i.e.

$$-\frac{\mathrm{d}V}{\mathrm{d}t} = \frac{p - p_{\mathrm{d}}}{R}, \tag{1}$$

where V is the GB volume, p is the GB pressure, R is the flow resistance, and p_{d}, the pressure in duodenum, is taken to be about 6 mmHg [20]. Assuming that the GB volume change rate, $\mathrm{d}V/\mathrm{d}t$, is related to the pressure drop rate $\mathrm{d}p/\mathrm{d}t$ [21],

$$\frac{\mathrm{d}V}{\mathrm{d}t} = C\frac{\mathrm{d}p}{\mathrm{d}t}, \tag{2}$$

where C is the constant compliance of the GB, we have

$$C\frac{\mathrm{d}p}{\mathrm{d}t} + \frac{p - p_{\mathrm{d}}}{R} = 0. \tag{3}$$

This is the same as the *Windkessel* model for the cardio-vascular system [22]. The general solution of this linear ordinary differential equation is

$$p = p_{\mathrm{d}} - (p_{\mathrm{d}} - p_{\mathrm{e}})\exp\left(\frac{t_{\mathrm{e}} - t}{RC}\right), \tag{4}$$

where p_{e} indicates the pressure when the GB has completely emptied, which is chosen to be $p_{\mathrm{e}} = 11$ mmHg [19], and t_{e} is the time taken for complete emptying. Complete emptying here

means that the GB volume V_e, at the end of emptying is $V_e = 0.3V_0$, where V_0 is the volume as the emptying begins. Here, we chose $V_e = 0.3V_0$ since it was found that in normal subjects a 30 min infusion of CCK-8 at rate of 60 ng/kg per hour causes a mean reduction in GB volume of 73% [20]. If a GB is impaired, then the time taken for complete emptying would be much longer than the normal emptying time of about 30 min, i.e. its emptying will be incomplete when refilling starts.

In general, the GB compliance, C, differs from one patient to another, but, as a first approximation, we take the average value measured by Middelfart *et al.* for human GB, $C = 2.731$ ml/mmHg [23].

2.2.2 Gallbladder volume change and ejection fraction. From (2)–(4), we can also solve for GB volume,

$$V = C(p_e - p_d)\exp\left(\frac{t_e - t}{RC}\right) + B, \tag{5}$$

where B is a constant, which is determined using the clinical measurements of GB volume at $(0, V_0)$ (t, V) and (t_e, V_e):

$$B = V_e - C(p_e - p_d), \tag{6}$$

Substituting (6) into (5) we have successively:

$$R = \left(\frac{t}{C}\right) \Big/ \ln\left\{\frac{V_0 - B}{V - B}\right\}, \tag{7}$$

and

$$t_e = \frac{t \ln\left[(V_0 - B)/(V_e - B)\right]}{\ln\left[(V_0 - B)/(V - B)\right]}. \tag{8}$$

These measurements also allow us to calculate the GB ejection fraction (EF) at 30 min after emptying as

$$\text{EF} = \frac{V_0 - V_{30}}{V} \times 100\%. \tag{9}$$

Note for subjects 33–37 (in table 1), the emptying is so fast that it stops before 30 min. For these cases, EF is not estimated from (9), but is simply set to be 100%.

2.2.3 Estimating the passive peak stresses. In order to estimate the peak stresses in GB muscle during emptying, we assume that the GB is an ellipsoid of homogeneous isotropic linear elastic material, with a thin uniform wall thickness, h_{GB}. The ellipsoid has a major axis D_1, and two minor axes, D_2 and D_3 ($D_1 \geq D_2 \geq D_3$). Using Cartesian coordinates as shown in figure 3, the mid-plane surface is described by

$$\begin{cases} x = 0.5D_1 \sin\theta\cos\varphi \\ y = 0.5D_2 \sin\theta\sin\varphi \,, \\ z = 0.5D_3 \cos\theta \end{cases} \tag{10}$$
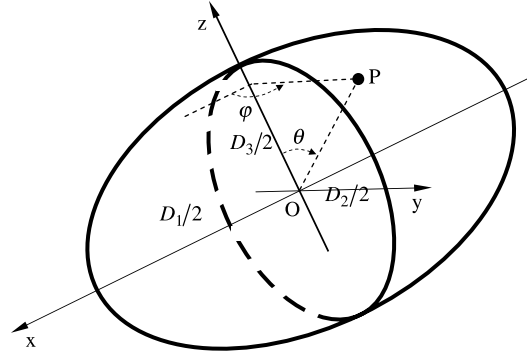
Figure 3. GB shape is assumed to be ellipsoidal during emptying, the major axis length is D_1, the minor axis length are D_2, and D_3 ($D_1 > D_2 \geq D_3$). The GB is subjected to a uniform internal pressure. The stress due to this pressure at a point P has three components: σ_θ (meridian), σ_φ (latitude), and $\tau_{\theta\varphi}$ (in surface).

where θ and φ are the two independent angular variables for a point position on the surface, and θ is in the meridian plane and measured from the positive z axis, $\theta \in [0, \pi]$; whereas, φ is in the latitude plane, which is perpendicular to z axis, and measured from the first quadrant of x–z plane, and $\varphi \in [0, 2\pi]$. The stresses in the ellipsoid surface under a uniform inner fluid pressure load p are given by [24],

$$
\begin{cases}
\sigma_\theta = \frac{pD_3 k_1 k_2}{4h_{GB}} \left[1 - \frac{k_1^2 - k_2^2}{k_1^2 k_2^2} \cos 2\varphi \right] F \\
\sigma_\varphi = \frac{pD_3}{4k_1 k_2 h_{GB}} \left[k_1^2 k_2^2 + \left(k_1^2 + k_2^2 - 2k_1^2 k_2^2 \right) \sin^2 \theta + \left(k_1^2 - k_2^2 \right) \cos^2 \theta \cos 2\varphi \right] \frac{1}{F}, \\
\tau_{\theta\varphi} = \frac{pD_3}{4k_1 k_2 h_{GB}} \left(k_1^2 - k_2^2 \right) \cos \theta \sin 2\varphi
\end{cases}
\tag{11}
$$

where $k_1 = D_1/D_3$, $k_2 = D_2/D_3$ and F is

$$
F = \frac{\sqrt{k_1^2 \cos^2 \theta \cos^2 \varphi + k_2^2 \cos^2 \theta \sin^2 \varphi + \sin^2 \theta}}{\sqrt{k_1^2 \sin^2 \varphi + k_2^2 \cos^2 \varphi}}.
\tag{12}
$$

The mean wall thickness of healthy human GB, h_{GB}, is taken to be 2.5 mm [25]. The maximum normal stress is then

$$
\sigma_{max} = \max[\sigma_\theta, \sigma_\varphi],
\tag{13}
$$

and the peak shear stress is

$$
\tau_{max} = \max[\tau_{\theta\varphi}]
\tag{14}
$$

To estimate the values of σ_{max} and τ_{max}, the GB domain was divided into 200×100 elements, and the values of the stresses were calculated from (11) at each node of the elements.

2.2.4 Contribution of the active normal stress. During emptying, the GB contracts due to CCK, which induces the active stress. In this study, for simplicity, we will assume that all
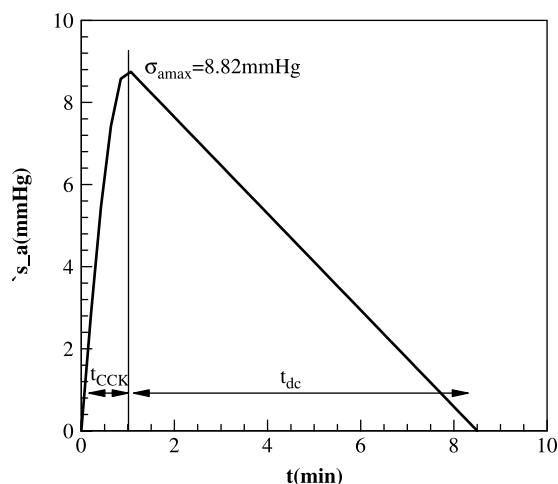
Figure 4. GB response curve to CCK [26]. t_{CCK} is the CCK response time, and t_{dc} is the CCK decay time, $\sigma_{a\,max}$ is the peak active stress.

patients experience the same level of CCK stimulation, which induces the same peak active normal stress. Thus, we use a uniform response curve to CCK, estimated from experiments [26], as shown in figure 4. This curve can be interpolated using

$$
\sigma_a = \begin{cases} \sigma_{a\,max} \sin\left(\frac{\pi t}{2 t_{CCK}}\right) & t \leq t_{CCK} \\ \sigma_{a\,max} \left(1 - \frac{t - t_{CCK}}{t_{dc}}\right) & t > t_{CCK} \end{cases} \tag{15}
$$

where $\sigma_{a\,max}$ is the maximum active stress taken to be 8.82 mmHg, t_{CCK} and t_{dc} are chosen to be $t_{CCK} = 1$ min and $t_{dc} = 7.5$ min [27]. There are no reports on active shear stress due to CCK. Finally, the total maximum normal stress in the GB wall during the emptying is thus

$$
\sigma_{t\,max} = \sigma_{a\,max} + \sigma_{max}. \tag{16}
$$

It is emphasized again that the contribution of the active stress in this model is assumed to be uniform for all patients. As active stress is highly likely to be patient and deformation dependent, better and more realistic modelling of this contribution is required in future.

3. Results

The clinical data for 37 patients during emptying were provided by the Royal Hallamshire Hospital, Sheffield, UK. Based on these data, we have calculated various factors, summarized in table 1.

All the initial GB volumes are in the range of 15–35 ml, except for those of subjects 19 and 37, which have an initial volume of 60 and 10 ml, respectively. The average initial GB volume is 25.3 ml. The GB volume change versus time is plotted in figure 5, for three typical subjects: 1, 18 and 37, which indicates, respectively, poor, fair and super-emptying behaviour.

34

W. G. *Li* et al.

Table 1. Major parameters of GB during emptying.

GB	V_0 (ml)	t (min)	EF (%)	R	D_1 (mm), k_1, k_2	p_{max} (mmHg)	$\sigma_{t\,max}$ (mmHg)	τ_{max} (mmHg)	Clinical observation
1	16.6		4.2	392.6	54.1, 2.31, 1.07	15.2	92.9	52.9	No pain
2	33.0		5.5	217.6	59.7, 2.01, 1.19	19.4	142.7	54.7	No pain
3	25.5		9.7	134.1	72.2, 2.81, 1.02	17.5	130.7	94.4	No pain
4	36.8		12.2	90.7	64.9, 2.01, 1.04	20.4	141.6	81.8	No pain
5	13.3		13.8	131.6	74.1, 4.49, 1.26	14.4	367.5	68.1	Pain
6	21.1		14.8	94.4	68.8, 3.31, 1.35	16.4	290.1	60.8	Pain
7	23.0		16.6	80.0	57.3, 2.34, 1.28	18.9	150.4	51.4	No pain
8	33.5		20.5	53.8	66.7, 2.52, 1.37	19.6	210.0	59.0	Pain
9	23.1		21.3	60.1	61.1, 2.97, 1.58	17.1	300.8	39.6	Pain
10	21.0		23.6	64.6	73.0, 3.65, 1.10	15.3	133.7	80.6	No pain
11	36.3		24.5	42.5	81.7, 3.35, 1.43	20.3	514.3	83.1	No pain
12	22.0		26.2	49.7	71.5, 3.26, 1.22	16.6	209.1	72.8	No pain
13	20.1		28.0	48.5	63.2, 3.07, 1.43	16.2	271.4	48.8	Pain
14	21.5		30.0	43.2	63.5, 3.41, 1.87	16.5	770.1	34.2	Pain
15	25.5		32.1	34.3	72.0, 2.82, 1.18	18.4	217.3	68.8	Pain
16	12.6		32.3	55.0	50.6, 2.42, 1.09	14.2	85.7	45.8	No pain
17	21.7		37.8	32.9	55.9, 2.06, 1.00	16.6	98.8	61.8	Pain
18	18.0		39.5	35.7	57.6, 2.02, 1.03	15.4	95.1	62.8	Pain
19	59.9		40.4	19.3	92.3, 2.66, 1.03	26.3	246.6	175.2	Pain
20	24.1		47.0	23.6	58.0, 2.12, 1.07	17.2	111.0	61.2	Pain
21	15.6		51.2	27.9	74.5, 2.64, 1.07	15.0	82.9	20.1	No pain
22	33.1		60.5	14	41.0, 1.69, 1.24	19.5	156.6	99.5	Pain
23	33.9		61.5	13.5	77.5, 3.18, 1.40	19.7	403.6	76.6	Pain
24	28.3		61.7	59.0	63.0, 2.42, 1.27	18.3	138.0	57.6	No pain
25	42.6		63.0	11.4	75.4, 2.62, 1.30	22.0	249.1	83.5	Pain
26	30.1		63.8	13.7	75.8, 3.08, 1.25	18.7	246.8	82.5	Pain
27	23.0	15	70.2	14.1	64.8, 2.61, 1.10	16.9	246.6	71.6	Pain
28	26.2	15	71.1	12.6	68.0, 2.61, 1.07	17.7	132.8	80.5	No pain
29	24.1	15	75.5	12.1	56.7, 2.02, 1.03	17.2	105.9	61.3	No pain
30	26.7	11	79.3	10.4	68.6, 2.85, 1.28	17.8	210.7	66.6	Pain
31	21.6	9	89.8	6.9	74.2, 3.84, 1.49	16.5	590.1	60.9	Pain
32	18.2	15	97.1	5.0	55.4, 2.30, 1.08	15.7	99.0	54.6	No pain
33	25.7	7	100.0	1.7	63.0, 2.24, 1.15	17.6	132.1	64.9	No pain
34	19.0	20	100.0	9.4	67.0, 3.66, 1.62	15.9	595.5	46.2	Pain
35	10.0	11	100.0	6.5	45.8, 2.65, 1.39	13.6	119.1	28.2	Pain
36	23.7	15	100.0	6.7	76.1, 3.34, 1.14	17.1	173.1	87.6	No pain
37	26.2	12	100.0	11.1	53.8, 1.78, 1.02	17.7	104.2	54.8	No pain

NB. For subjects 33–37, emptying is finished before 30 min. EF for these subjects is taken to be 100%.
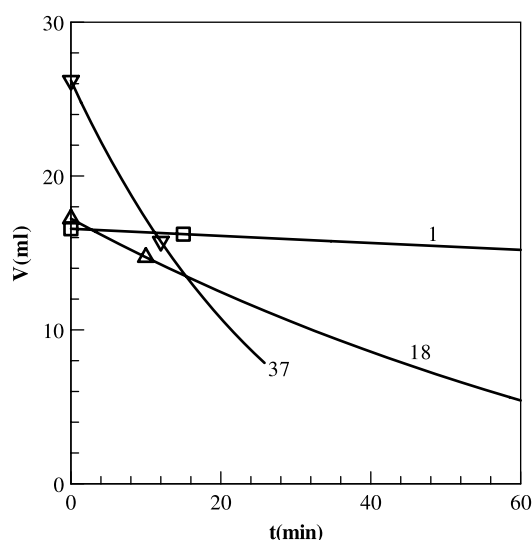
Figure 5. GB volume variation with time during emptying for 3 typical subjects. The symbols are the experimental data and the solid curves are from (5).

The flow resistance varies from 1.7 to 392.6 mmHg/ml per minute, showing a significant variation across the subjects. The subjects with good emptying (large EF) have low flow resistance and those with poor emptying (small EF) usually present high resistance. In general, the resistance is in the range of 20–70 mmHg/ml per minute. The average resistance is 53.4 mmHg/ml per minute, however the resistances of subjects 1–3, and 5 are all higher than 130 mmHg. The resistance of the cystic duct of the prairie dog is found to increase from 50 to 120 mmHg/ml per minute when its GB changed from healthy status to that with gallstones after feeding with a cholesterol diet [28]. Thus if we can extend the experimental finding for prairie dogs to human, then it is likely that these with higher resistances indicate the unhealthy states.

The maximum values of the pressure, p_{max}, for all subjects are given in table 1 and the pressure variation with time is illustrated in figure 6 for subjects 1, 18 and 37. It can be seen that the peak pressure of most of the GBs, except GB 19, is in the range of 15–20 mmHg. This agrees well with physiological values [20]. The GB pressure of subjects 1–14, which have poor emptying, decreases more slowly with time. In general, the flatness of the pressure curves seems to be associated with poor emptying. In other words, a GB with poor-emptying is subject to a higher pressure for a longer period of time.

The GB shapes in the subject group in table 1 can be characterized by two main geometric types: those (type 1) for which the ellipsoid is elongated with $k_2 > 1$; and those (type 2) for which the ellipsoid is a spheroid and $k_2 \approx 1$. The peak normal stress level of first type is higher than that of second type; see figure 7 for subjects 12 (type 1, $k_2 = 1.22$) and 17 (type 2, $k_2 = 1.0$). The shear stress patterns for these two subjects are similar, with the maximum/minimum values occurring at the same orientation: $\theta = \varphi = 45°$, but are very different to the normal stresses. This is because the maximum value of the normal stress is much more sensitive to the geometric changes, therefore, its location and value can differ significantly for different geometric types.

When these factors are compared with the pain information from clinical observations in table 1, it shows that the direct correlations with pain of the flow resistance, shear stress, and
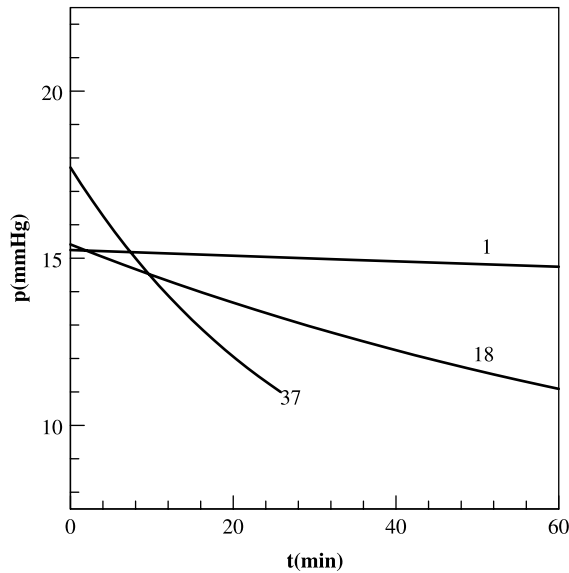
Figure 6.   The pressure variation with time during emptying for subjects 1, 18 and 37, respectively.

EF are all rather poor. The maximum pressure, p_{max}, seems to be weakly correlated with pain. The most remarkable correlation, however, is found to be with the maximum normal stress $\sigma_{t\,max}$.

In the following, we consider three pain predictors based on (1) ejection fraction: EF $<$ 35%, which is commonly used in clinics, (2) pressure: $p > 15.4$ mmHg (15.4 mmHg is estimated when patients' average EF is 35%) and (3) maximum normal stress: $\sigma_{t\,max} > \sigma*$, where $\sigma* = 200$ mmHg is from an average value calculated from pressure measurement by Gaenseler [11]. The results of the predictions are listed in tables 2–4.

From table 3, it is clear that all predictions using $\sigma_{t\,max}$ are correct except for GBs 11, 12, 17, 18, 20, 22 and 35, thus out of 37 cases, 30 agree with the clinical observations. For comparison, if we use EF $<$ 35% as the pain threshold, the results are far less positive, with less than half agreeing with clinical data. The correlations of the shear stress and resistance are also poor to pain. The results from using $p > 15.4$ mmHg is better than using EF, but not as good as using $\sigma_{t\,max}$.

In order to see how reliable these predictions are, below we analyse these from a more rigorous statistical standpoint, making use of the logistic transformation (see appendix A).

Table 5 is the 2×2 contingency table for the three pain related indices, EF, p_{max} and $\sigma_{t\,max}$, where the counts of the success and failure based on clinical observations are listed. The corresponding success and failure rates are also listed in brackets. It can be seen that the success rates of positive (pain) and negative (no pain) predictions using EF is all less than 0.5. Therefore, this index has no prediction power and should be rejected.

The success rates of the positive and negative predictions using p_{max} are somewhere between 0.5 and 0.7. Interestingly, the rate of its negative prediction is better than the positive prediction. However, for $\sigma_{t\,max}$ both (positive and negative) the success rates are over 0.75, with the positive (pain) prediction as high as 0.882.

The 95% confidence intervals for the success rate of pain and no pain predictions are shown in table 6. The difference between the success rates of positive and negative
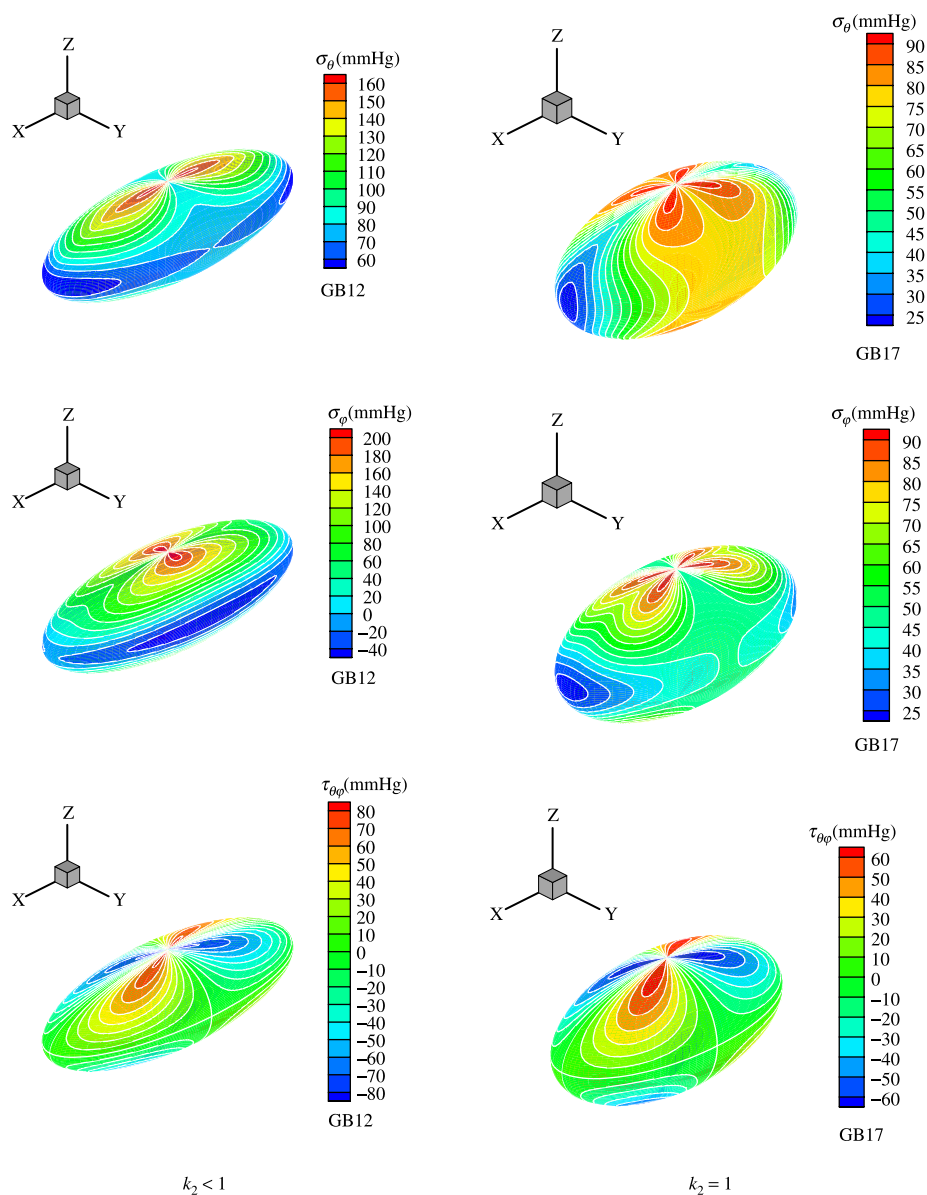
Figure 7. The stress contours on the GB wall at the start of emptying for subjects 12 (left) and 17 (right). The top frame is the principal stress σ_θ, the middle frame is the principal stress σ_φ, and the bottom one is the shear stress $\tau_{\theta\varphi}$.

predictions can be seen by using the ratio of odds from the two rows in the 2×2 contingency table (see table 5). The inference for the odds ratio of positive (pain) and negative (no pain) predictions is summarized in table 7 for both p_{max} and $\sigma_{t\ max}$. The 95% confidence interval for odds ratio of success rate of positive (pain) and negative (no pain) prediction with p_{max} is (0.60, 0.769) i.e. using this index, the success rate of pain prediction is at least 23.1% less than no pain prediction. Whilst with $\sigma_{t\ max}$ this is (1.373, 1.605), thus the

Table 2.   GB pain prediction using bile EF.

GB	EF (%)	Pain prediction	Clinical observation	Agreement
1	4.2	Positive	Negative	No
2	5.5	Positive	Negative	No
3	9.7	Positive	Negative	No
4	12.2	Positive	Negative	No
5	13.8	Positive	Positive	Yes
6	14.8	Positive	Positive	Yes
7	16.6	Positive	Negative	No
8	20.5	Positive	Positive	Yes
9	21.3	Positive	Positive	Yes
10	23.6	Positive	Negative	No
11	24.5	Positive	Negative	No
12	26.2	Positive	Negative	No
13	28.0	Positive	Positive	Yes
14	30.0	Positive	Positive	Yes
15	32.1	Positive	Positive	Yes
16	32.3	Positive	Negative	No
17	37.8	Negative	Positive	No
18	39.5	Negative	Positive	No
19	40.4	Negative	Positive	No
20	47.0	Negative	Positive	No
21	51.2	Negative	Negative	Yes
22	60.5	Negative	Positive	No
23	61.5	Negative	Positive	No
24	61.7	Negative	Negative	Yes
25	63.0	Negative	Positive	No
26	63.8	Negative	Positive	No
27	70.2	Negative	Positive	No
28	71.1	Negative	Negative	Yes
29	75.5	Negative	Negative	Yes
30	79.3	Negative	Positive	No
31	89.8	Negative	Positive	No
32	97.1	Negative	Negative	Yes
33	100.0	Negative	Negative	Yes
34	100.0	Negative	Positive	No
35	100.0	Negative	Positive	No
36	100.0	Negative	Negative	Yes
37	100.0	Negative	Negative	Yes

success rate of pain prediction is 37.5% higher than no pain prediction. This is important as in clinical diagnosis, the significance of a reliable positive prediction is much greater than that of a negative prediction. Therefore, we believe that the peak normal stress is the better pain prediction compared with the maximum pressure (table 7).

4. Discussions

Our study shows that the peak normal stress is a good index to use for pain prediction. This prediction is correct for all but seven subjects (table 4) in all 37 cases studied. A reason for the seven failed cases could be that these patients have slightly lower or higher pain threshold levels than the standard value used. It is also likely to be the simplifications introduced in the model, such as a uniform GB compliance, and an elliptical GB shape, which are used in the model for every subject, whereas in reality, should all be subject-dependent.

Table 3. GB pain prediction using the peak pressure.

GB	p_{max} (mmHg)	Pain predicted	Clinical observation	Agreement
35	13.6	Negative	Positive	No
16	14.2	Negative	Negative	Yes
5	14.4	Negative	Positive	No
21	15.0	Negative	Negative	Yes
1	15.2	Negative	Negative	Yes
10	15.3	Negative	Negative	Yes
18	15.4	Positive	Positive	Yes
32	15.7	Positive	Negative	No
34	15.9	Positive	Positive	Yes
13	16.2	Positive	Positive	Yes
6	16.4	Positive	Positive	Yes
14	16.5	Positive	Positive	Yes
31	16.5	Positive	Positive	Yes
12	16.6	Positive	Negative	No
17	16.6	Positive	Positive	Yes
27	16.9	Positive	Positive	Yes
9	17.1	Positive	Positive	Yes
36	17.1	Positive	Negative	No
20	17.2	Positive	Positive	Yes
29	17.2	Positive	Negative	No
3	17.5	Positive	Negative	No
33	17.6	Positive	Negative	No
28	17.7	Positive	Negative	No
37	17.7	Positive	Negative	No
30	17.8	Positive	Positive	Yes
24	18.3	Positive	Negative	No
15	18.4	Positive	Positive	Yes
26	18.7	Positive	Positive	Yes
7	18.9	Positive	Negative	No
2	19.4	Positive	Negative	No
22	19.5	Positive	Positive	Yes
8	19.6	Positive	Positive	Yes
23	19.7	Positive	Positive	Yes
11	20.3	Positive	Negative	No
4	20.4	Positive	Negative	No
25	22.0	Positive	Positive	Yes
19	26.3	Positive	Positive	Yes

It is important to realise that the peak normal stresses in GB wall not only depend on the pressure p, but also on its geometry, D_1, D_2 and D_3, and their relative ratios, see table 1. In fact, we believe that it is through the normal stress mechanism that the effects from both the pressure and the geometry change come into play in producing pain. Additionally, it is interesting to note that a poor emptying rate (a lower ejection fraction) is not necessarily associated with the pain, subjects 1–4, 7 and 10–12 have all showed poor emptying, but do not experience any pain, both from the model prediction, or from the clinical observation. The GBs with super emptying (a larger ejection fraction value) can also demonstrate pain, for instance, subjects 31 and 34. Therefore, the ejection fraction is not considered to be a good indicator for pain prediction. This is important since impaired GB emptying is still used as the clinical criterion for cholecystectomy [1]. Our study clearly suggests that this criterion needs to be reviewed.

However, we should point out that there are limitations in our current approach. We have assumed here that the GB is an ellipsoid, which is a commonly adopted assumption in clinical

Table 4.   Pain prediction using the peak normal stress.

GB	$\sigma_{t\,max}$ (mmHg)	Pain predicted	Clinical observation	Agreement
21	82.9	Negative	Negative	Yes
16	85.7	Negative	Negative	Yes
1	92.9	Negative	Negative	Yes
18	95.1	Negative	Positive	No
17	98.8	Negative	Positive	No
32	99.0	Negative	Negative	Yes
37	104.2	Negative	Negative	Yes
29	105.9	Negative	Negative	Yes
20	111.0	Negative	Positive	No
35	119.1	Negative	Positive	No
3	130.7	Negative	Negative	Yes
33	132.1	Negative	Negative	Yes
28	132.8	Negative	Negative	Yes
10	133.7	Negative	Negative	Yes
24	138.0	Negative	Negative	Yes
4	141.6	Negative	Negative	Yes
2	142.7	Negative	Negative	Yes
7	150.4	Negative	Negative	Yes
22	156.6	Negative	Positive	No
36	173.1	Negative	Negative	Yes
12	209.1	Positive	Negative	No
8	210.0	Positive	Positive	Yes
30	210.7	Positive	Positive	Yes
15	217.3	Positive	Positive	Yes
19	246.6	Positive	Positive	Yes
27	246.6	Positive	Positive	Yes
26	246.8	Positive	Positive	Yes
25	249.1	Positive	Positive	Yes
13	271.4	Positive	Positive	Yes
6	290.1	Positive	Positive	Yes
9	300.8	Positive	Positive	Yes
5	367.5	Positive	Positive	Yes
23	403.6	Positive	Positive	Yes
11	514.3	Positive	Negative	No
31	590.1	Positive	Positive	Yes
34	595.5	Positive	Positive	Yes
14	770.1	Positive	Positive	Yes

practice (e.g. in real-time Ultrasonography). However, this approximation can cause an error up to 10% in estimates of GB size [29]. Our model can be improved if the GB volume can be obtained more accurately, which may be possible with improved clinical instrumentation. Another limitation is that we have assumed that GB behaves as a homogenous linear isotropic elastic material. Future work is required to estimate the importance and influence

Table 5.   Counts of the success rate of positive (pain) and negative (no pain) prediction by using the three predictors.

Predictor	Prediction	Success	Failure	Sample size
EF	Positive (pain)	7(0.438)	9(0.562)	16
	Negative (no pain)	8(0.381)	13(0.619	21
p_{max}	Positive (pain)	18(0.581)	13(0.219)	31
	Negative (no pain)	4(0.667)	2(0.333)	6
$\sigma_{t\,max}$	Positive (pain)	15(0.882)	2(0.118)	17
	Negative (no pain)	15(0.75)	5(0.25)	20

Table 6.   95% confidence intervals of the success rate of positive (pain) and negative (no pain) prediction.

Predictor	Success rate of positive (pain) and negative (no pain) prediction	Confidence interval
EF	0.438	(0.225, 0.677)
	0.381	(0.203, 0.598)
p_{max}	0.581	(0.405, 0.739)
	0.667	(0.268, 0.916)
$\sigma_{t\,max}$	0.882	(0.631, 0.970)
	0.75	(0.522, 0.892)

Table 7.   Inference for the odds ratio of positive (pain) and negative (no pain) prediction.

Predictor	Odds ratio of sample	Asymptotic standard error of sample	95% confidence interval for odds ratio with normal distribution
p_{max}	-0.386	-0.063	(0.60, 0.769)
$\sigma_{t\,max}$	0.396	-0.0395	(1.375, 1.605)

of nonlinearity and anisotropy on the stress calculations. We have also assumed a uniform thickness of GB wall, which may also bring in some degree of inaccuracy in our predictions. Detailed measurement of the thickness changes, especially when GB wall is in contraction, is required before any further analysis can be carried out. In addition, although this model has included both active and passive stresses, the active stress is not obtained from the smooth muscle mechanics, rather it is taken to be the same typical form for all subjects applied uniformly over the GB wall. In practice, this also varies with individual subject. There should be a range of values for the threshold stress at which patients can feel pain, *i.e.* the pain sensitivity is individual. Using a standard value of 200 mmHg here is only an approximation. Finally, the number of clinical samples that we have been able to use over the last few years is still relatively small, being 37 only. For a more reliable pain prediction, more samples should be included. Further and more extensive studies from our and other groups are clearly required. Much greater knowledge about the smooth muscle function in the GB, remodelling and growth during abnormal emptying, and the mechanical sensor related to the pain, as well as the individual pain threshold, are all required in order to understand the precise mechanism of the GB pain.

Having mentioned all these limitations, it is encouraging that a simple model based on non-invasive clinical measurement (volume changes) may be used to predict the pain with 88.2% positive success rate for the samples studied. However, although, this study suggests that a simple model can provide a good first approximation to this complicated problem, more extensive studies on a wide range of patients under more controlled conditions (on age and gender) are clearly required to confirm this.

5. Conclusions

In this paper, a simple GB model is developed to evaluate the correlations of the mechanical factors with GB pain, based on clinical data for 37 patients. These factors include the GB

pressure, ejection fraction, flow resistance, shear stress, and peak shear and normal stresses. It is found that the peak normal stress is the best mechanical factor that may be used to predict the GB pain. Using this as a pain criterion, the agreement with 37 clinical observations (for positive prediction) is about 88.2%. On the other hand, it is found that, a poor emptying, the maximum pressure in GB, the peak shear stress, and the flow resistance, do not correlate directly with pain. This is because the normal stress in GB wall depends not only on the GB pressure (*i.e.* flow resistance), but also on the GB geometry. Although this is simple model and has only been tested for 37 patients, its simplicity, and the fact that it requires the minimum clinical data, makes it a promising potential as one of the routine clinical diagnostic methods.

Acknowledgements

References

[1] Shaffer, E., 2003, Acalculous biliary pain: new concepts for an old entity, *Digestive and Liver Disease*, **35**(Suppl 3), S20–S25.
[2] Corazziari, E., Shaffer, E.A., Hogan, W.J., Sherman, S. and Toouli, J., 1999, Functional disorders of the biliary tract and pancreas, *Gut*, **45**(Suppl II), II48–II54.
[3] Rastogi, A., Slivka, A., Moser, A.J. and Wald, R., 2005, Controversies concerning pathophysiology and management of acalculous biliary-type abdominal pain, *Digestive Diseases and Sciences*, **50**(8), 1391–1401.
[4] Williamson, R.C.N., 1988, Acalculous disease of gall bladder, *Gut*, **29**, 860–872.
[5] Smythe, A., Majeed, A.W., Fitzhenry, M. and Johnson, A.G., 1998, A requiem for the cholecystokinin provocation test?, *Gut*, **43**, 571–574.
[6] Funch-Jensen, P., 1995, Sphincter of Oddi physiology, *Journal of Hepato-Biliary–Pancreatic Surgery*, **2**, 249–254.
[7] Bingener, J., Richards, M.L., Schwesinger, W.H. and Sirinek, K.R., 2004, Laparoscopic cholecystectomy for biliary dyskinesia, *Surgical Endoscopy*, **18**, 802–806.
[8] Yap, L., Wycherley, A.G., Morphett, A.D. and Toouli, J., 1991, Acalculous biliary pain: cholecystectomy alleviates symptoms in patients with abnormal cholescintigraphy, *Gastroenterology*, **101**, 786–793.
[9] Smythe Ahmed, R., Fitzhenry, M., Johnson, A.G. and Majeed, A.W., 2004, Bethanechol provocation testing does not predict symptom relief after cholecystectomy for acalculous biliary pain, *Digestive and Liver Disease*, **36**, 682–686.
[10] Ness, T.J. and Gebhart, G.F., 1990, Visceral pain: a review of experimental studies, *Pain*, **41**, 167–234.
[11] Gaensler, E.A., 1951, Quantitative determination of the visceral pain threshold in man, *Journal of Clinical Investigation*, **30**, 406–420.
[12] Csendes, A., Kruse, A., Funch-Jensen, P., Oster, M.J., Ornsholt, J. and Amdrup, E., 1979, Pressure measurements in the biliary and pancreatic duct systems in controls and in patients with gallstones, previous cholecysterctomy, or common bile duct stones, *Gastroenterology*, **77**, 1203–1210.
[13] Drewes, A.M., Pedersen, J., Liu, W., Arendt-Nielsen, L. and Gregersen, H., 2003, Controlled mechanical distension of human oesophagus: sensory and biomechanical findings, *Scandinavica Journal of Gastroenterology*, **38**, 27–35.
[14] Barlow, J.D., Gregersen, H. and Thompson, D.G., 2001, Identification of the biomechanical factors associated with the perception of distension in the human esophagus, *American Journal of Physiology*, **282**, G683–G689.
[15] Petersen, P., Gao, C., Arendt-Nielsen, L., Gregersen, H. and Drewes, A.M., 2003, Pain intensity and biomechanical response during ramp-controlled distension of the human rectum, *Digestive Diseases and Sciences*, **48**(7), 1310–1316.

[16] Gao, C., Arendt-Nielsen, L., Liu, W., Petersen, P., Drewes, A.M. and Gregersen, H., 2002, Sensory and biomechanical responses to ramp-controlled distension of the human duodenum, *American Journal of Physiology*, **284**, G461–G471.

[17] Gregersen, H., Hausken, T., Yang, J., Odegaard, S. and Giljia, O.H., 2006, Mechanosensory properties in the human gastric antrum evaluated using B-mode ultrasonography during volume-controlled antral distension, *American Journal of Physiology*, **290**, G876–G882.

[18] Cozzolino, H.J., Goldstein, F., Greening, R.R. and Wirts, C.W., 1963, The cystic duct syndrome, *JAMA*, **185**, 920–924.

[19] Majeed, A.W., Smythe, A. and Johnson, A.G., 1994, Continuous *in vivo* manometry of the human gallbladder, *Neurogastroenterology and Motility*, **6**(2), 162–165.

[20] Dodds, W.J., Hogan, W.J. and Green, J.E., 1989, Motility of the biliary system. In: S.G. Schultz (Ed.) *Handbook of Physiology: The Gastrointestinal System* (Betheda, Maryland: American Physiological Society), **vol. 1**, Section 6, Part 2(28), pp. 1055–1101.

[21] Ryan, J. and Cohen, S., 1976, Gallbladder pressure–volume response to gastrointestinal hormones, *American Journal of Physiology*, **230**, 1461–1465.

[22] Fung, Y.C., 1984, *Biodynamics Circulation* (New York: Springer-Verlag), pp. 22–23.

[23] Middelfart, H.V., Jensen, P., Hojgaard, L. and Funch-Jensen, P., 1998, Pain patterns after distension of the gallbladder in patients with acute cholecystis, *Scandinavica Journal of Gastroenterology*, **33**, 982–987.

[24] Novozhilov, V.V., 1964, *Thin Shell Theory* (Groningen: P. Noordhoff Ltd), pp. 125–130.

[25] Deitch, E.A., 1981, Uitility and accuracy of ultrasonically measured gallbladder wall as a diagnostic criteria in biliary tract disease, *Digestive Diseases and Sciences*, **26**(8), 686–693.

[26] Matsumoto, T., Sarna, S.K., Condon, R.E., Dodds, W.J. and Mochinaga, N., 1988, Canine gallbladder cyclic motor activity, *American Journal of Physiology*, **255**, G409–G416.

[27] Milenov, K. and Shahbazian, A., 1995, Cholinergic pathways in the effect of motilin on the canine ileum and gallbladder motility: *in vivo* and *in vitro* experiments, *Comparative Biochemistry Physiology*, **112A**(3/4), 403–410.

[28] Pitt, H.A., Doty, J.E., DenBesten, L. and Kuchenbecker, S.L., 1981, Stasis before gallstone formation: altered gallbladder compliance or cystic duct resistance, *The American Journal of Surgery*, **143**, 144–149.

[29] Everson, G.T., Braverman, D.Z., Johnson, M.L. and Kern, F., 1980, A critical evaluation of real-time ultrasonography for the study of gallbladder volume and contraction, *Gastroenterology*, **79**, 40–46.

[30] Inglfinger, J.A., Mosteller, F., Thibodeau, L.A. and Ware, J.H., 1987, *Biostatistics in Clinical Medicine* (New York: Macmillan Publishing Co. Inc.), pp. 140–148.

[31] Dawson-Saunders, B. and Trapp, R.G., 1994, *Biostatistics* (London: Prentice-Hall International Inc.), pp. 148–149.

Appendix A: logistic transformation [30,31]

From elementary statistics, we know that if we have a sample from a normal distribution with known variance σ^2, a 95% confidence interval for the mean μ is [31]

$$\bar{x} \pm 1.96 \frac{\sigma}{\sqrt{n}}. \tag{A1}$$

The quantity $\sigma/\sqrt{n}$ is called the standard error; it measures the variability of the sample mean $\bar{x}$ about the true mean μ. The number 1.96 comes from a table of the standard normal distribution; the area under the standard normal density curve between -1.96 and 1.96 is 95%.

The confidence interval (A1) is valid because over repeated samples the estimate $\bar{x}$ is normally distributed about the true value μ with a standard deviation of $\sigma/\sqrt{n}$.

When the sample size is small, we may be able to improve the quality of the approximation by applying a suitable reparameterization, a transformation of the parameter to a new scale. The "logistic" or "logit" transformation is such a transformation, defined as

$$\phi = \log\left(\frac{p}{1 - p}\right). \tag{A2}$$

Here, $0 \leq p \leq 1$ and $-\infty < \phi < -\infty$. Solving (A2) for p produces the back-transformation,

$$p = \frac{e^{\phi}}{1 + e^{\phi}}. \tag{A3}$$

Table A1 shows a 2×2 contingency table for the two variables A and B, with sample sizes n_1 (success) and n_2 (failure), and B with sample sizes n_3 (success) and n_4 (failure), respectively. We want to determine the endpoints of 95% confidence interval for success rates p_1 and p_2 as well as to compare them. The success rates are calculated from

$$p_1 = \frac{n_1}{n_1 + n_2}, \tag{A4}$$

and

$$p_2 = \frac{n_3}{n_3 + n_4}. \tag{A5}$$

The endpoints of the 95% confidence intervals for success rate p_1 are

$$p_{1\,\text{low}} = \frac{e^{p_1 - 1.96\sqrt{1/(p_1(n_1+n_2)(1-p_1))}}}{1 + e^{p_1 - 1.96\sqrt{1/(p_1(n_1+n_2)(1-p_1))}}}, \tag{A6}$$

and

$$p_{1\text{high}} = \frac{e^{p_1 + 1.96\sqrt{1/(p_1(n_1+n_2)(1-p_1))}}}{1 + e^{p_1 + 1.96\sqrt{1/(p_1(n_1+n_2)(1-p_1))}}}. \tag{A7}$$

The endpoints of 95% confidence interval for success rate p_2 (variable B) are

$$p_{2\text{low}} = \frac{e^{p_2 - 1.96\sqrt{1/(p_2(n_3+n_4)(1-p_2))}}}{1 + e^{p_2 - 1.96\sqrt{1/(p_2(n_3+n_4)(1-p_2))}}}, \tag{A8}$$

and

$$p_{2\text{high}} = \frac{e^{p_2 + 1.96\sqrt{1/(p_2(n_3+n_4)(1-p_2))}}}{1 + e^{p_2 + 1.96\sqrt{1/(p_2(n_3+n_4)(1-p_2))}}}. \tag{A9}$$

The difference between success rate of A and B can be distinguished by using the ratio of odds from the two rows in table A1. The asymptotic standard error of two samples is [30]

$$\sigma = \log\left(\sqrt{\frac{1}{n_1} + \frac{1}{n_2} + \frac{1}{n_3} + \frac{1}{n_4}}\right), \tag{A10}$$

and the ratio of odds from two samples is [30]

$$\theta = \log\left[\frac{p_1(1 - p_2)}{(1 - p_1)p_2}\right]. \tag{A11}$$

Table A1. 2 × 2 contingency table for the variables *A* and *B*.

Variable	Success	Failure	Sample size
A	$n_1(p_1)$	$n_2(1 - p_1)$	$n_1 + n_2$
B	$n_3(p_2)$	$n_4(1 - p_2)$	$n_3 + n_4$

The endpoints of 95% confidence interval for the ratio of odds are [30]

$$\theta_{\text{low}} = e^{\theta - 1.96\sigma}, \tag{A12}$$

and

$$\theta_{\text{high}} = e^{\theta + 1.96\sigma} \tag{A13}$$